EVALUATION OF CONSTITUTIVE MODELS IN PREDICTING RATCHETING RESPONSES OF A STRUCTURE UNDER THERMO-MECHANICAL LOADINGS

J. MACEDO[*,1,2], J. M. BERGHEAU[2], E. FEULVARCH[2], H. BATTIE[1,2], O. ANCELET[1], A. MARTIN[1], STÉPHANE CHAPULIOT[3]

[1] Engineering and Design Authority Unit
Framatome
France
email: jean-caio.macedo-alves-de-lima1@framatome.com
/olivier.ancelet@framatome.com/antoine.martin@framatome.com

[2] University of Lyon, EC-Lyon, LTDS, UMR5513 CNRS
Saint-Etienne, France
email: jean-michel.bergheau@enise.fr/eric.feulvarch@enise.fr/hugo.battie@enise.fr

[3] EDF Group
France
email: stephane.chapuliot@edf.fr

Key words: Ratcheting, cyclic plasticity, thermo-mechanical loadings, constitutive models, induction heating

Abstract.

Ratcheting is a damage mechanism that needs to be avoided to ensure the structural integrity. To this end, the use of a constitutive model is sometimes required. The objective of this paper is to evaluate the performance of three constitutive models in predicting ratcheting responses of a 316L stainless steel structure under thermo-mechanical loadings.

Firstly, the bi-tube test is described, including specimen geometry, heating system and mechanical loading. Secondly, the models proposed by Prager, Armstrong-Frederick and Chaboche are briefly recalled and a methodology to identify their parameters is presented.

Finally, a finite element model is exposed and numerical simulations are carried out in order to compare and discuss the results of the above mentioned constitutive models. Comparisons demonstrate that the best option to simulate ratcheting responses seems to be the introduction of an isotropic hardening with a plastic strain memorization in the cyclic plasticity model. It has also been observed that the ratcheting rate has to be considered during the model identification phase.

1 INTRODUCTION

The plastic strain may accumulate through the cycles, when a structure is subjected to a cyclic loading with non-zero mean stress. If the accumulation of plastic strain ceases after few cycles, we consider that a structure reached a shakedown. However, if the plastic strain continues progressively to grow, the structure undergoes ratcheting.

In engineering design codes for components and structures, it is necessary to demonstrate that certain limits of plastic strain are not exceeded and that the plastic strain growth rate decreases asymptotically to zero throughout the service life of a structure. Hence, shakedown is accepted if the plastic strains does not exceed the allowed one. Nevertheless, ratcheting is not allowed because the accumulated plastic strain may lead to failure by a loss of functionality or a damage interaction. [1]

Two types of method are often used in order to assess this phenomenon. The first method; also called simplified one, performs generally an elastic finite element analysis (FEA) to predict ratcheting. As plasticity is not considered, this method is overly conservative. The second evaluates the plastic strain by a direct cycle-by-cycle elastic-plastic FEA. On the one hand, this method is less conservative, on the other hand, it is more computationally expensive than the first one. Moreover, the capabilities of a constitutive model to simulate ratcheting responses are not well known.

To better understand the ratcheting phenomenon, this article evaluates the performance of three cyclic plasticity models for local ratcheting responses simulations of a structure. The section 2 describes the experimental study known as bi-tube test. The section 3 describes the finite element model. The constitutive models and a methodology to identify their parameters are also presented. The Section 4 is dedicated to magneto-thermal and mechanical analyses of the bi-tube test. Finite element calculations are exposed and simulations are carried out in order to evaluate the constitutive models. Finally, section 5 concludes with suggestions for future work.

2 BI-TUBE TEST

2.1 Principle of the test

Bi-tube test is inspired by Uga's works [2] who carried out the first fundamental experiment to investigate the ratcheting: the three bars specimen. Uga's test is very limited in terms of applied loadings. In fact, due to the bar slenderness, Uga's specimen is sensitive to the buckling phenomenon. To mitigate this limitation, Taleb [3] proposes replacing the bars specimen with cylinders.

The experiment is carried out on two thin concentric cylinders rigidly fixed at their ends to have an identical axial displacement (figure 1). The loading can be split into a constant tensile force and a cyclic heating/cooling. Concerning cyclic heating by induction, the outer tube is heated while the inner tube is maintained at room temperature. Furthermore, the constant tensile force is in fact an axial stress applied to both tubes.

The principle of the test is the following: during the heating phase the outer structure expands. Since the apparatus is constrained to have the same axial displacement, the inner tube is in tensile whereas the outer one is in compression. Figure 2 perfectly depicts this principle, by focusing on a section view of the two concentric tubes.

Finally, the structures are cooled down by natural convection and axial conduction. Hence, the combination of an axial thermal gradient cyclic loading and a constant tensile force (mean stress) may induces the local ratcheting.

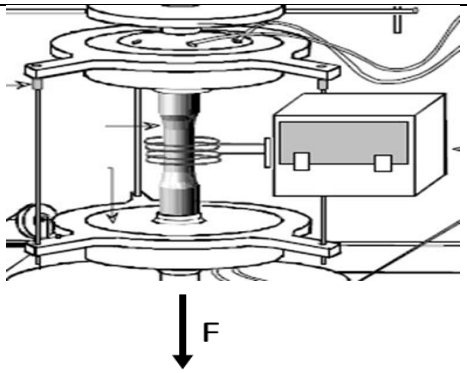

Figure 1: Apparatus test

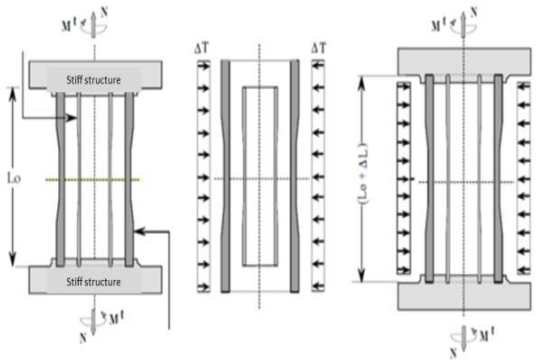

Figure 2: Principle of the test

2.2 Specimen material and geometry

The specimens are made of 316L austenitic stainless steel. This material is commonly used in pressurized piping in nuclear power plants. Figures 3 and 4 show the comparison between the monotonic and cyclic curves of bi-tube and nuclear piping materials at 20°C, 300°C and 450°C. It can be seen that bi-tube material is harder than piping one for the monotonic curves. Concerning the cyclic curves, bi-tube and nuclear piping materials are very similar at 20°C. However, piping material is harder than bi-tube at 300°C. The difference between them is less significant as the strain increases.

The bi-tube structure is composed of two concentric tubes, as it was aforementioned. Their dimensions are presented in figure 5. It can be seen that the outer tube is thinner than the inner one. This choice was made in order to maximize the axial thermal gradient stress.

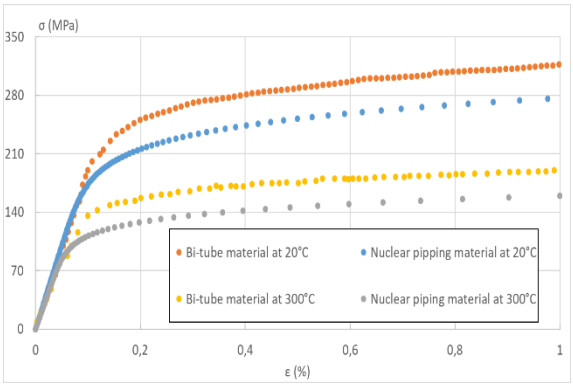

Figure 3: 316L monotonic curves

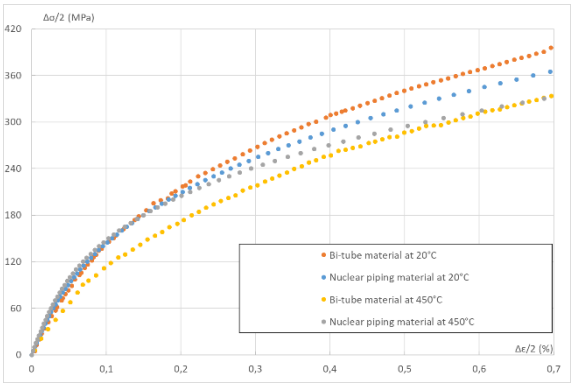

Figure 4: 316L cyclic curves

2.3 Thermo-mechanical loading

Thermal loading: The outer tube is submitted to an induction heating by four coils. After 80 seconds, when the outer structure reaches 350°C, the heating is stopped and the cooling by natural convection starts. During all test, the internal wall of the inner tube is air conditioned to keep this tube at room temperature. One thermal cyclic takes about 600 seconds.

Mechanical loading: An axial force is applied in order to obtain an axial stress of 120 MPa on the thinnest part of the tubes [4].

Instrumentation: Thermocouples are placed on the specimens to quantify the thermal loading. Figure 6 shows time-measured temperature curve of the outer specimen in the middle section. This curve is used, in this study, to develop the numerical model. To measure the axial strain accumulation (or axial ratcheting), a strain gauge is placed in the middle section of the inner tube. The measured strain, at the end of each cycle, over twenty-two cycles is given in figure 7.

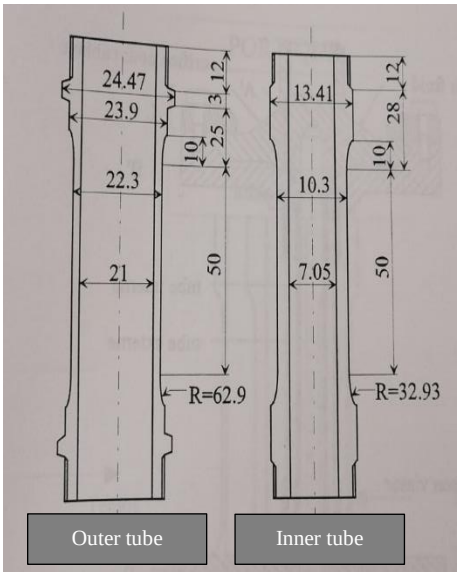

Figure 5: Bi-tube specimens

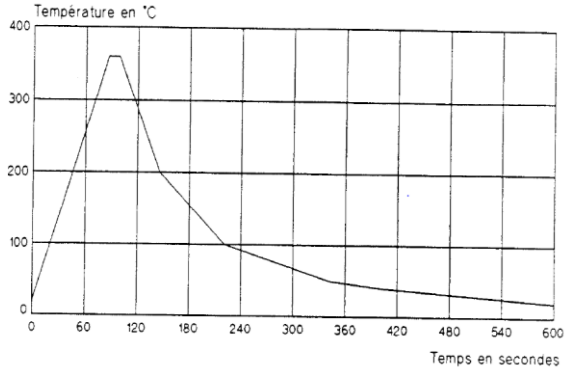

Figure 6: Measured temperature of the outer specimen in middle section

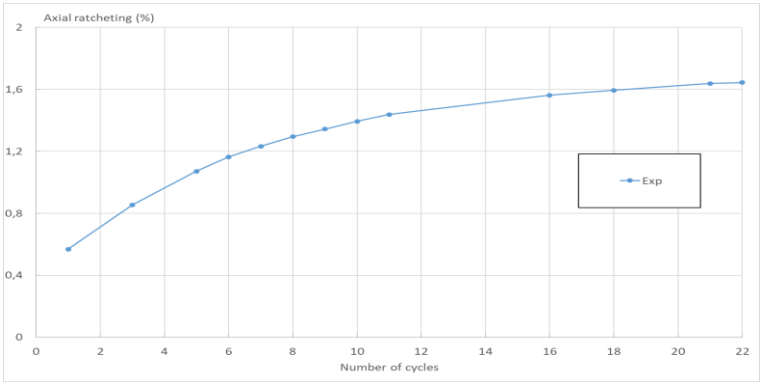

Figure 7: Axial ratcheting in the inner tube

3 NUMERICAL SIMULATION

3.1 Finite element model

Due to the axisymmetric model, a 2D finite element model (figure 8) is meshed with *Visual mesh* software from ESI Group [5]. Due to the symmetrical conditions, half of a meridional section is considered. The yellow and red parts are the inner and the outer tubes, respectively. The blue element represents the empty zone between the two tubes and the coils are represented by the green parts.

First of all, the induction heating simulation is performed. From this simulation, the temperature map of the bi-tube test is obtained. Once this simulation validated, the thermo-mechanical one is carried out. The thermal loading is thus set using the temperature cards of the magneto-thermal analysis. Moreover, elastic-plastic models are used in order to simulate the material behaviour.

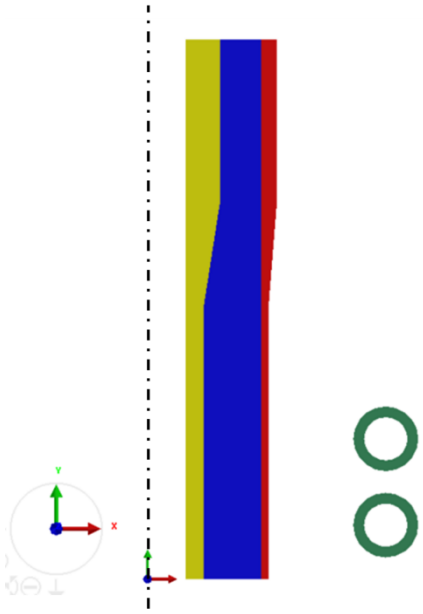

Figure 8: Finite element model

3.2 Induction heating simulation

The induction heating simulation is performed using a coupled model with *SYSTUS* from ESI Group. Indeed, the resolution of the magneto-dynamic problem and the thermal one is coupled by the power dissipation by the Joule effect and the dependence of the electromagnetic properties with temperature. This problem is not solved using a direct method, but using an iterative one. To do so, the followings assumptions are made:

- Thermal time (or macro time) and electromagnetic time (or micro time) are decoupled
- The power dissipated by the Joule effect is considered as an average over an electromagnetic half-period in the current thermal time step
- In a thermal time step t, the state of equilibrium is achieved when the difference between successive temperatures are sufficient small

This iterative method is presented in figure 9. The full mathematical formulation of magneto-dynamic-thermal coupling is described in [6].

Thermal proprieties of 316L austenitic steel stainless such as the thermal conductivity, the volumetric mass, and specific heat capacity are taken from [7]. The electrical conductivity, which is an electromagnetic property, is plotted on figure 10. Moreover, void and bi-tube permeabilities are equal to μ_0 and $1.1\mu_0$, respectively.

The boundary conditions are considered as follows and showed in figure 12:

- The natural convection is represented by a convection coefficient (h_{air}); a temperature (T_{air}) and the boundary element method (BEM) [8].
- The air conditioning system is described by a convection coefficient ($h_{air\ condi}$) and a temperature ($T_{air\ condi}$)
- Air properties are affected to the empty zone (the blue elements)
- Induction heating is represented by a frequency and a voltage applied to the coils.

As creep is not significant, a last assumption is made: the range in which the temperature is maintained constant is not simulated.

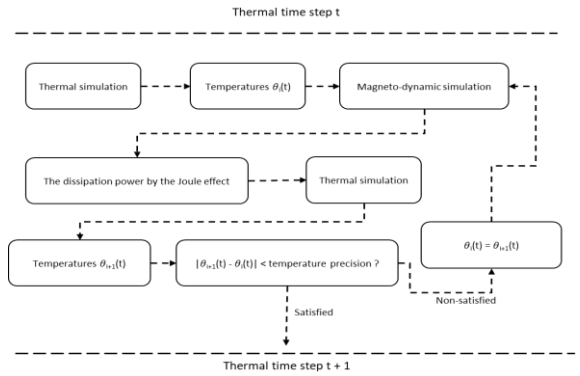

Figure 9: Iterative method for coupling magneto-dynamic with thermal simulation

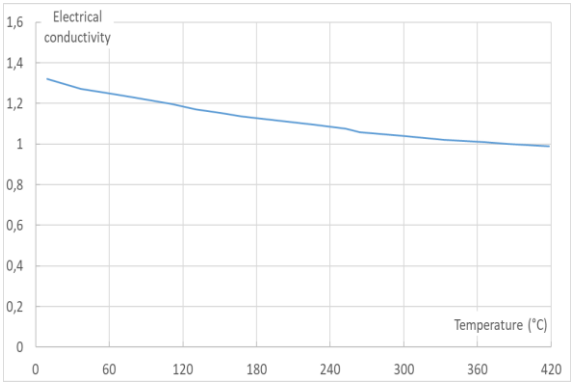

Figure 10: Electrical conductivity of the 316L material

3.3 Thermo-mechanical simulation

3.3.1 Constitutive models

Prager [9] proposed a model that the plastic modulus calculation is coupled with its kinematic hardening rule through the consistency condition (Eq (1)). This model is also called the linear kinematic hardening model.

$$d\underline{\underline{X_{PR}}} = \frac{2}{3} C\ d\underline{\underline{\varepsilon^p}} \tag{1}$$

Then, Armstrong-Frederick [10] introduce a recall term in the Prager model to make the rule nonlinear (Eq (2)). This is also called the nonlinear kinematic hardening model.

$$d\underline{\underline{X_{AF}}} = \frac{2}{3} C\ d\underline{\underline{\varepsilon^p}} - \gamma \underline{\underline{X_{AF}}} dp \tag{2}$$

For uniaxial loading with non-zero mean stress, these models produce a shakedown or a constant ratcheting rate (Eq (3)), respectively, when the steady state is achieved. As a results, these models are not robust enough to simulate local or global ratcheting.

$$\Delta\varepsilon^{p}_{ratcheting} = \frac{1}{\gamma}\ln\left(\frac{X^{2}_{\min} - \left(\frac{C}{\gamma}\right)^{2}}{X^{2}_{\max} - \left(\frac{C}{\gamma}\right)^{2}}\right) \tag{3}$$

The three improved models presented below are based on the abovementioned ones. They have been proposed in order to better simulate the cyclic plasticity. Their performances in simulating local ratcheting are evaluated in this paper.

Double Armstrong-Frederick model: This model which is also referenced as 2AF in this study is a superposition of two Armstrong-Frederick hardening rules. This superposition was first recommended and popularised by Chaboche. This model is given as follows:

$$\begin{cases} d\underline{\underline{X}} = d\underline{\underline{X_{AF1}}} + d\underline{\underline{X_{AF2}}} \\ d\underline{\underline{X_{AF1}}} = \frac{2}{3}C_1\, d\underline{\underline{\varepsilon^{p}}} - \gamma_1 \underline{\underline{X_{AF1}}}\, dp \\ d\underline{\underline{X_{AF2}}} = \frac{2}{3}C_2 d\underline{\underline{\varepsilon^{p}}} - -\gamma_2 \underline{\underline{X_{AF2}}}\, dp \end{cases} \tag{4}$$

Note that as two nonlinear kinematic hardening are considered, the models is well-known for producing a constant ratcheting rate.

Armstrong-Frederick- Prager model: This model which is also mentioned here as AF-Prager is also a superposition of two kinematic hardening rules with a value of γ_2 sets to 0. The combination of a linear and non-linear kinematic hardening reduces the ratcheting rate. As a consequence, this model simulates better the ratcheting than the abovementioned one.

Simplified version of the Chaboche model: The simplified version of the Chaboche model which is called CHA in this work is a combination of the AF-Prager model and the isotropic hardening rule with a plastic strain range memorization [11]. The incorporation of an isotropic hardening rule introduces the cyclic hardening/softening of the material. This hardening rule is defined as follows:

$$\begin{cases} dR = b(Q - R)dp \\ Q = Q_M - (Q_0 - Q_M)\exp(-2\beta q) \end{cases} \tag{5}$$

Where the parameter q is the plastic strain range memorization calculated on the non-hardening surface. b and β are two parameters depending on mainly the material. Their values are not determined in this study, but taken from the literature.

3.3.2 Parameters identifications

Bi-tube material curves (figures 3 and 4) are used to determinate the model's parameters. Models using kinematic hardening are identified by fitting the uniaxial monotonic curves while the simplified version of the Chaboche model is determined by fitting the uniaxial monotonic and the uniaxial cyclic curves, simultaneously. In fact, the isotropic hardening is obtained from the uniaxial cyclic curves. Furthermore, two identifications were performed to both the AF-Prager and the CHA models for comparing the influences of their parameters on the ratcheting simulation.

To avoid any possible errors and to find the best fit, a Python program based on the least-squared regression was developed to perform these identifications. The following table gives the parameter set of all model at 20°C. It should be observed that Q_0 has negative values. In fact, the 316L austenitic stainless steel softens slightly if it is submitted to low values of the plastic strain amplitude. This behaviour is thus modelled by a negative value of Q_0. Figure 11 shows the comparison between experimental monotonic curve and simulations at 20°C.

Tableau 1: Parameter sets at 20°C

Model	k (MPa)	C_1 (MPa)	γ_1	C_2 (MPa)	γ_2	Q_0 (MPa)	Q_M (MPa)	b	β
2AF	195,16	15440.64	171.54	136145.5	2506.06				
AF-Prager 1	207,62	77729.03	1248.64	6056.70	0				
CHA 1	207,62	77729.03	1248.64	6056.70	0	-83.21	653.18	15	30
AF-Prager 2	207,62	40496.90	561.50	2694.20	0				
CHA 2	207,62	40496.90	561.50	2694.20	0	-29.22	463.51	15	30

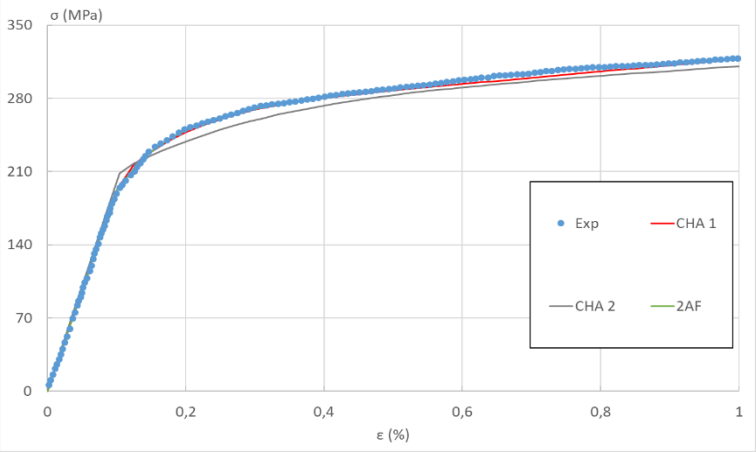

Figure 11: Monotonic curve - Comparison between experimental result and simulations

3.3.3 Thermo-mechanical simulation

Thermo-mechanical simulations, using the abovementioned constitutive models, are performed by elasto-plastic FEA for calculating the axial ratcheting. The thermal expansion and Young's modulus are taken from [7]. The boundary conditions and the loadings are considered as follows and given in figure 13:

- Axial displacement of the low section (violet line) is blocked
- Axial displacement of the upper section (dark line) have the same displacement
- Axial stress applied to the upper section (dark line)
- Thermal loadings
- Blue and green elements are not included in the modelling

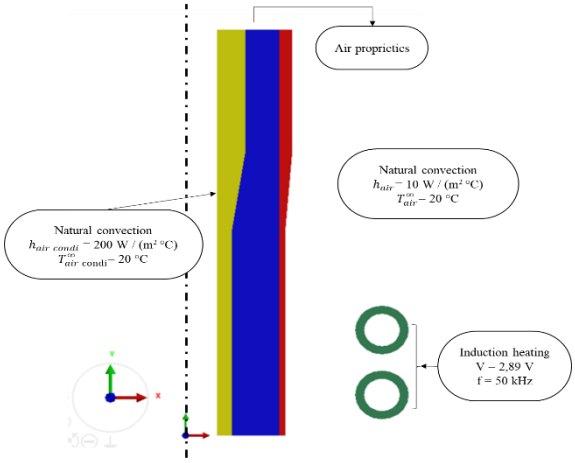

Figure 12: Thermal boundary conditions

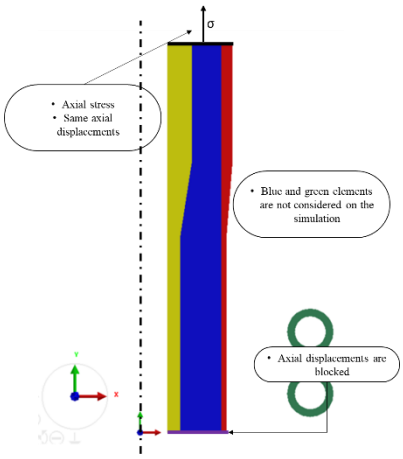

Figure 13: Mechanical boundary conditions

4 RESULTS AND DISCUSSIONS

4.1 Validation of thermal loading

The voltage V and the frequency of induction f are determined in order to have a correct reproducibility of thermal loading. A sensitivity analysis was performed to determinate the best parameter set of V and f. The parameters V and f determined are 2.89V and 50kHz, respectively. Figure 14 shows the comparison between the experimental result and the simulation. Knowing that the experimental curve is plotted using six points, one can considerate that the numerical simulation gives results in good agreement with the experiment. Beside of this, figure 15 presents the temperature distribution of the bi-tube structure which is in accordance with the experimental observations. This thermal result is thus used in the thermo-mechanical simulation.

4.2 Comparison between constitutive models

Figure 16 shows the comparison of axial ratcheting between experimental results and simulations. As it was abovementioned, the axial ratcheting of the 2AF model gives a linear ratcheting when the steady state is achieved. Thus, this model has a tendency to over-predict the experimental ratcheting. AF-Prager 1 and CHA 1 models under-predicted widely the axial ratcheting. This underestimation is mainly caused by the high value of C_1 and γ_1. In fact, the ratcheting rate depends on these parameters and it can be deduced from Eq (3) that the higher the value of C_1 (and γ_1), the smaller is the ratcheting rate.

Realizing that, a second identification was made using AF-Prager and CHA models. For this

new identification, the values of C_1 and γ_1 are approximately two times smaller than the first one. The comparison between the first determinations and the second ones is given in figure 17. One can see that the second identifications simulate better the ratcheting than the first one. Considering only the second identification, CHA 2 predicts better the experimental result than the AF-Prager 2. Indeed, the ratcheting rate of AF-Prager 2 is greater than CHA 2 and experimental result (figure 18). Thus, it indicates that the incorporation of an isotropic hardening rule improves the simulation of ratcheting.

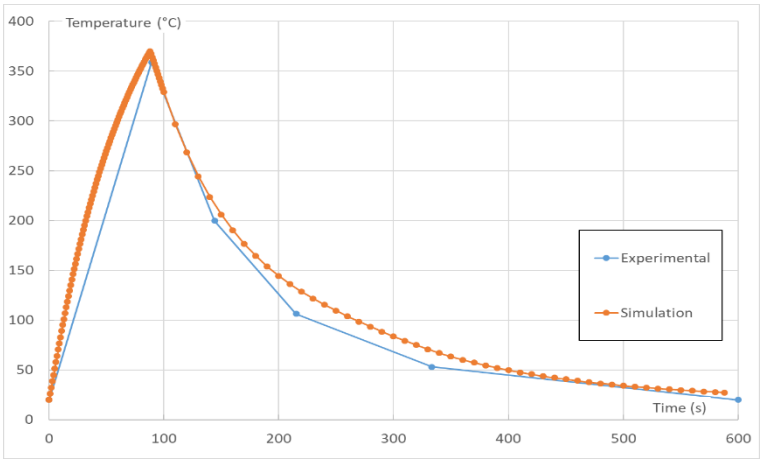

Figure 14: Comparison between the experimental temperature and the simulation

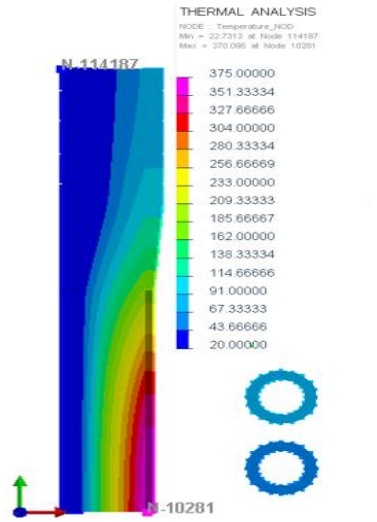

Figure 15: Temperature distribution at the maximum temperature

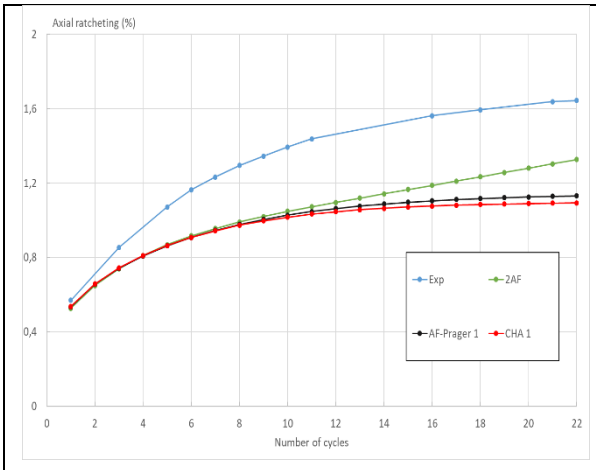

Figure 16: Axial Ratcheting - Comparison between the experimental result and simulations - First parameter sets

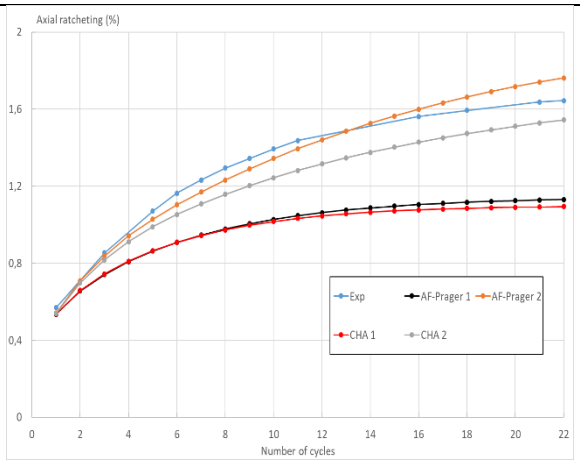

Figure 17: Axial Ratcheting - Comparison between the experimental result and simulations - First vs second parameter sets

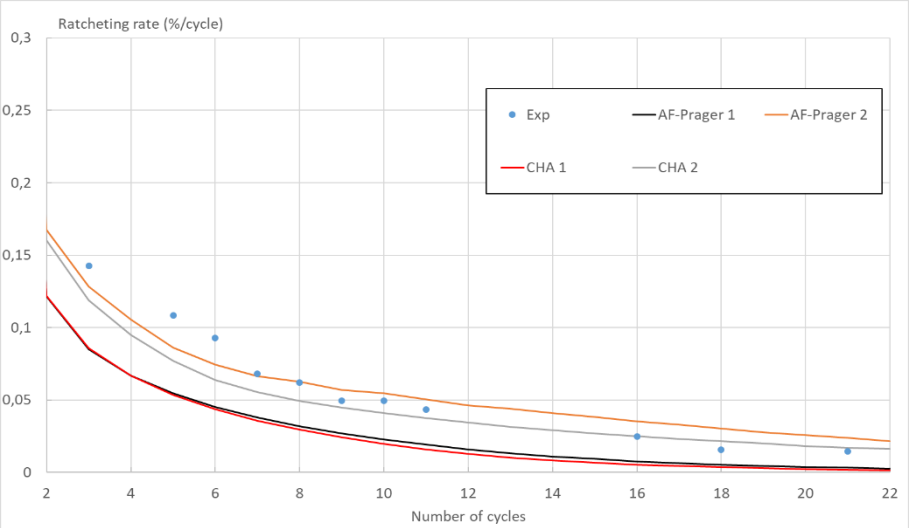

Figure 18: Ratcheting rate - Comparison between the experimental result and simulations - Chaboche model

5 CONCLUSIONS

This paper evaluates three constitutive models in simulating the ratcheting of the bi-tube test. The bi-tube best is a ratcheting experiment developed by Taleb [3] in order to better understand the local ratcheting.

The thermo-mechanical simulations of this experiment were then performed with Armstrong-Frederick-Prager, double Armstrong-Frederick and the simplified version of Chaboche models. The parameter determination is made using material curves. Before to perform this thermo-mechanical simulation, it was necessary to simulate and calibrate the thermal loading. This modelling provided a correct estimation of the thermal phenomenon.

With the first model parameter set, none of the aforementioned models could well predict the experimental results. In fact, all models underestimated the bi-tube's strain accumulation. The definition of ratcheting rate was used to understand the underestimation in simulating the ratcheting response. As C_1 and γ_1 coefficients, for all models, were taken sufficient large, the ratcheting rate was taken extremely small.

A second parameter set of AF-Prager and CHA model was thus determined considering both material curves and ratcheting rate. From that identification, the calculation has shown acceptable results for the CHA 2 model. The average relative error between the latter and test curves was equal to 8%.

The results presented in this paper demonstrate that the considerable advancements in cyclic plasticity modelling have made improvements in the ratcheting simulations. However, cautions have been taken throughout the parameters determination phase. It was observed that it is extremely important to consider both the material curves and ratcheting rate for achieving well ratcheting simulations.

The next step is to evaluate the previous models in predicting multiaxial ratcheting to demonstrate that they are able to simulate both local and global ratcheting with a good accuracy. From all these results, it will then be possible to develop some novel simplified criteria to assess

ratcheting damage.

REFERENCES

[1] J. Macedo, S. Chapuliot, J. M. Bergheau, E. Feulvarch, O. Ancelet and A. Martin, "A historical review of design analyses and experimental observations of ratcheting phenomenon," *Pressure Vessels & Piping Conference*, 19-24 July 2020.

[2] T. Uga, "An experimental study on thermal-stress ratcheting of austenitic stainless steel by a tree bars specimen," *Nuclear engineering and design*, pp. 326 - 335, April 1973.

[3] L. Taleb, "Structure métallique sous un chargement thermomécanique cyclique - Effet des surcharges mécaniques de courte durée," Thesis, INSA Lyon, 1991.

[4] O. Philip, "Structure métallique sous un chargement thermomécanique cyclique - Interaction déformation progressive-fluage," Thesis, INSA Lyon, 1996.

[5] ESI GROUP, Multiphysics Engineering Simulation, https://www.esi-group.com/fr.

[6] J. M. Bergheau and R. Fortunier, Finite Element Simulation of Heat Transfer, France, 2004.

[7] AFCEN, French design and construction rules for mechanical components of nuclear installations: high temperature, research and fusion reactors, 2018.

[8] J.-M. Bergheau and P. Conraux, "FEM-BEM coupling for the modelling of induction heating processes including moving parts," *Proc. of 1st Int. Conf. On Thermal Process Modelling and Computer Simulation*, Vols. E-5, no. 1, pp. 91-99, march 2000.

[9] W. Prager, "Non Isothermal Plastic Deformation," *Koninlijke Nederlandse Akademic van Wetenschapen*, vol. 61, pp. 176-182, 1958.

[10] P. J. Armstrong and C. O. Frederick, "A Mathematical Representation of the Multiaxial Bauschinger Effect,," Berkeley Nuclear Laboratories,1966, Reprinted in Mat. High Temp. 24, 2007, 11-26.

[11] J.-L. Chaboche, "a Review of some Plasticity and Viscoplasticity Constitutive Theories," *International Journal of Plasticity*, pp. 1642-1693, 2008.